Electron-Impact Ionization of Atomic Ions in the Na Isoelectronic Sequence

M. S. Pindzola, D. M. Mitnik, and J. A. Shaw
Department of Physics, Auburn University, Auburn, AL 36849, USA

D. C. Griffin
Department of Physics, Rollins College, Winter Park, FL 32789, USA

N. R. Badnell and H. P. Summers
Department of Physics and Applied Physics, University of Strathclyde, Glasgow G4 0NG, UK

D. R. Schultz
Controlled Fusion Atomic Data Center, Physics Division, Oak Ridge National Laboratory, Oak Ridge, TN 37831, USA

A database is assembled which contains electron-impact ionization rate coefficients for selected atomic ions in the Na isoelectronic sequence. The rate coefficients are obtained from a Maxwellian convolution of distorted-wave cross sections which include direct ionization of the 2p and 3s subshells, as well as inner-shell excitations from the 2s and 2p subshells leading to autoionization. These excitation-autoionization contributions can be large for many Na-like atomic ions. To assist modeling efforts of moderately dense plasmas, the rate coefficients are resolved as to the final state of the ionization process. A sample database file is presented for Fe^{15+}. The complete database will reside in electronic form at the Controlled Fusion Atomic Data Center at ORNL (http://www-cfadc.phy.ornl.gov/data_and_codes/).

I. INTRODUCTION

Concurrent with the development of sophisticated models of the dynamics of atomic ions in laboratory and astrophysical plasmas has been the increased demand for more accurate and extensive atomic collision data. Cooperation between the plasma modeling and atomic collision communities is enhanced when accurate and extensive atomic databases are generally available and easy to use. Plasma modeling needs, as expressed in the extent and level of accuracy of the database, can serve as a focus for theoretical and experimental efforts in atomic collision physics. On the other hand, the generation of a certain key atomic cross section or rate coefficient to high accuracy can be as computationally or observationally demanding as the overall plasma modeling. In that light, the database serves as a valuable resource to be husbanded and then applied to gain a better understanding of atomic processes in plasmas.

In this paper we assemble a database which contains electron-impact ionization rate coefficients for selected atomic ions in the Na isoelectronic sequence. A good review of the theoretical and experimental work on the ionization cross sections for both light and heavy Na-like atomic ions is found in Moores and Reed [1]. We begin construction of the database at the transition metal ions; i.e. Ti, Cr, Fe, and Ni. For maximum predictive power over a variety of plasma conditions, current collisional-radiative modeling codes [2] require J level resolved ionization rate coefficients. Since most atomic collision experiments count charge-changing events and thus sum over all final states of the ion, we have extensively modified the distorted-wave codes developed in support of those experiments to generate final state resolved ionization cross sections and rate coefficients. In this regard, the plasma modeling codes are much more demanding on atomic collision theory than the current atomic collision experiments. In the following paragraphs we first review distorted-wave theory as applied to the electron-impact ionization of atomic ions in Sec. II, and then present a sample database file for Fe^{15+} in Sec. III. We summarize our plans for the extension of the database to other isoelectronic sequences in Sec. IV.

II. THEORY

Major contributions to the electron-impact single-ionization cross section are made by the following two processes:

$$e^- + A^{q+} \rightarrow A^{(q+1)+} + e^- + e^- \ , \tag{1}$$

and

$$e^- + A^{q+} \rightarrow (A^{q+})^* + e^- \rightarrow A^{(q+1)+} + e^- + e^- \ , \tag{2}$$

where A represents an arbitrary ion with charge q. The first process is direct ionization while the second is excitation-autoionization. The total ionization cross section is given by:

$$\sigma_T(g \rightarrow f) = \sigma_{DI}(g \rightarrow f) + \sigma_{EA}(g \rightarrow f) \ , \tag{3}$$

where $\sigma_{DI}(g \rightarrow f)$ is the direct ionization cross section and $\sigma_{EA}(g \rightarrow f)$ is the excitation-autoionization cross section from an initial level g of the N-electron ion to a final level f of the (N-1)-electron ion. The excitation-autoionization cross section through inner-shell excitation to an intermediate autoionizing level j is given by:

$$\begin{aligned} \sigma_{EA}(g \rightarrow f) &= \sum_j \sigma_E(g \rightarrow j) \left[\frac{A_a(j \rightarrow f) + \sum_i A_r(j \rightarrow i) B_a(i \rightarrow f)}{\sum_k A_a(j \rightarrow k) + \sum_i A_r(j \rightarrow i)} \right] \\ &\equiv \sum_j \sigma_E(g \rightarrow j) B_a(j \rightarrow f) \ , \end{aligned} \tag{4}$$

where $\sigma_E(g \rightarrow j)$ is the excitation cross section from level g to level j, $A_a(j \rightarrow k)$ is the autoionizing rate from level j to level k, $A_r(j \rightarrow i)$ is the radiative rate from level j to any lower energy level i, and $B_a(j \rightarrow f)$ is the multiple or effective branching ratio for autoionization from level j to level f, defined by the term in large square brackets. This term contains in turn the effective branching ratio $B_a(i \rightarrow f)$ for further (secondary) autoionization from level i to level f. Thus the effective autoionization branching ratios are defined by the recursive expression:

$$B_a(i \rightarrow f) \equiv \left[\frac{A_a(i \rightarrow f) + \sum_{n<i} A_r(i \rightarrow n) B_a(n \rightarrow f)}{\sum_k A_a(i \rightarrow k) + \sum_{n<i} A_r(i \rightarrow n)} \right] \ . \tag{5}$$

This allows one to take into account all the possible secondary autoionizations following cascading, until the radiative decay reaches a level m below the first ionization limit such that $B_a(m \rightarrow f) = 0$.

A theoretical calculation of the total electron-impact ionization cross section for an arbitrary ion divides into three parts. The first part is a collisional ionization calculation for σ_{DI}, the second part is a collisional excitation calculation for σ_E, and the third part is an atomic structure calculation for B_a. The Maxwellian rate coefficients for an atomic database are then separately calculated and catalogued for σ_{DI} and σ_{EA}.

The direct ionization cross sections are first calculated in a configuration average distorted-wave approximation, which is described in detail in the proceedings of a NATO Advanced Study Institute [3]. The configuration average cross sections are resolved as to initial and final LSJ levels by purely algebraic transformations [4]. Experimental threshold energies are then incorporated using a simple energy scaling of the resolved cross sections.

Inner-shell excitation cross sections are calculated in a multi-configuration J level resolved distorted-wave approximation. For some years we have calculated inner-shell excitation cross sections using an LSJ level resolved collisional excitation code [5] based on Cowan's HFR atomic structure program [6]. For this project we have written a new LSJ level resolved collisional excitation code based on Fischer's MCHF atomic structure package [7]. We also employ an jjJ level resolved collisional excitation code [8] based on the relativistic atomic structure code RELAC [9].

The branching ratios for autoionization are calculated in a configuration interaction LSJ level resolved distorted-wave approximation using the AUTOSTRUCTURE code [10,11]. We also employ an extended version of RELAC [12] to calculate the autoionization and radiative rates needed for branching ratios. For current plasma modeling codes the branching ratios need to be resolved as to the final J level. On the other hand, for comparisons with atomic collision experiments that measure charge-changing events, only branching ratios summed over all final states are required (i.e. $\sum_f B_a(j \rightarrow f)$).

The J level resolved ionization cross sections are entered into the atomic database in the form of Maxwell-averaged rate coefficients. The numerical entry format is that developed for ADAS [2,13]. Future updates are made easier by separately cataloging rate coefficients for direct ionization and excitation-autoionization.

III. ELECTRON-IMPACT IONIZATION OF Fe^{15+}

Our example from the ionization database for the Na isoelectronic sequence is Fe^{15+}. The Maxwellian rate coefficients for direct ionization of Fe^{15+} (seq='Na', nucchl=26) are presented in Table I for the transitions $2s^22p^63s\ ^2S_{\frac{1}{2}} \rightarrow 2s^22p^6\ ^1S_0, 2s^22p^53s\ ^3P_{2,1,0}$, and $2s^22p^53s\ ^1P_1$. The initial (nlev) and final (nprf) levels are identified by configuration, spin multiplicity (S), orbital angular momentum (L), and total angular momentum (WJ). The ionization potentials (bwni, bwnf) and level splittings (wni, wnf) are in cm^{-1}. The direct ionization rates in cm^3 sec^{-1} from each initial level (indi, in this case 1) to each final level (indf, in this case 5) are tabulated as a function of electron temperature (Te) in Kelvin. The data entry is signed and dated at the bottom with a short description of the theoretical procedure used to generate the atomic data.

Excitation-autoionization cross sections are presented in Figure 1 for the transitions $2s^22p^63s\ ^2S_{\frac{1}{2}} \rightarrow 2s^22p^53s3\ell\ ^{2,4}L_J$. There are 43 J levels in the $2s^22p^53s3\ell$ configurations, with additional correlation provided by the $2s^22p^53p^2$, $2s^22p^53p3d$, and $2s^22p^53d^2$ configurations. The dashed curves are perturbative-relativistic distorted-wave calculations based on the MCHF atomic structure code [7] and the solid curves are fully-relativistic distorted-wave calculations based on the RELAC atomic structure code [9]. The number of partial waves included is sufficient to guarantee convergence of the cross-section. The upper curves are cross sections in which all of the branching ratios have been set to unity, while the lower curves show a depletion of the ionization cross section when radiation damping is included. For this moderately charged atomic ion, we find excellent agreement between the perturbative-relativistic and fully-relativistic calculations.

Excitation-autoionization cross sections are presented in Figure 2 for the transitions $2s^22p^63s\ ^2S_{\frac{1}{2}} \rightarrow 2s^22p^53sn\ell\ ^{2,4}L_J (n = 3,4,5,6)$ and $2s2p^63sn\ell\ ^{2,4}L_J (n = 3,4)$. Both curves are fully-relativistic distorted-wave calculations, the solid curve with radiation damping and the dashed curve without radiation damping. Our complete excitation-autoionization cross section calculations are in excellent agreement with previous theoretical work [14,15], and when added to our direct ionization cross section calculations are in reasonable agreement with ion-storage ring experiments [15]. The Maxwellian rate coefficients for indirect ionization, obtained using the radiation-damped cross sections, are presented in Table II. Since all of the inner-shell autoionizing levels included in the calculations lie below the $2s^22p^53s$ ionization thresholds, there are only indirect contributions to the $2s^22p^6\ ^1S_0$ level. Finally, we present the Maxwellian rate coefficient for the total electron-impact ionization of Fe^{15+} in Figure 3. The additional enhancement due to excitation-autoionization is found to be quite substantial over a wide temperature range.

IV. SUMMARY

Electron-impact ionization rate coefficients have been calculated in the distorted-wave approximation for transition metal ions in the Na isoelectronic sequence. A database consisting of two parts has been assembled: (1) direct ionization rate coefficients and (2) indirect ionization rate coefficients. The two parts can be easily combined to yield total ionization rate coefficients resolved as to the final ionized level. Examples of the various database formats have been given for the electron ionization of Fe^{15+}. The complete database in electronic form resides at the Controlled Fusion Atomic Data Center at Oak Ridge National Laboratory in the USA (http://www-cfadc.phy.ornl.gov/data_and_codes/).

In the future we plan to extend the ionization rate coefficient database to include transition metal ions in the Mg isoelectronic sequence. Excitation-autoionization contributions for these ions are quite large [16]; both for the ground $3s^2\ ^1S_0$ and metastable $3s3p\ ^3P_{0,2}$ levels. A parallel effort is also underway to assemble a database which contains final J level resolved radiative and dielectronic recombination rate coefficients for those atomic ions of key importance to laboratory and astrophysical plasma research.

V. ACKNOWLEDGMENTS

This work was supported in part by the U.S. Department of Energy under Grant No. DE-FG05-86-ER53217 with Auburn University, Grant No. DE-FG05-93-ER54218 with Rollins College, Contract No. DE-AC05-84OR21400 with Oak Ridge National Laboratory, by the U.K. EPSRC under Contract GR/K/14346 with the University of Strathclyde.

[1] D. L. Moores and K J Reed, Adv. Atm. Mol. Opt. Phys **34**, 301 (1994).
[2] H. P. Summers, Adv. Atm. Mol. Opt. Phys. **33**, 275 (1993).
[3] M. S. Pindzola, D. C. Griffin, and C. Bottcher, in *Atomic Processes in Electron-Ion and Ion-Ion Collisions*, ed. F. Brouillard, NATO ASI B **145**, 75 (1986).
[4] D. H. Sampson, Phys. Rev. A **34**, 986 (1986).
[5] D. C. Griffin, M. S. Pindzola, and C. Bottcher, Phys. Rev. A **36**, 3642 (1987).
[6] R. D. Cowan, *The Theory of Atomic Structure and Spectra*, (U. Calif. Press, 1981).
[7] C. F. Fischer, Comput. Phys. Commun. **64**, 369 (1991).
[8] A. Bar-Shalom, M. Klapisch, and J. Oreg, Phys. Rev. A **38**, 1773 (1988).
[9] Developed by M. Klapisch, A. Bar-Shalom, and E. Luc-Koenig, based on the parametric potential method of M. Klapisch, Comput. Phys. Commun. **2**, 239 (1971).
[10] W. Eissner, M. Jones, and H. Nussbaumer, Comput. Phys. Commun. **8**, 270 (1974).
[11] N. R. Badnell, J. Phys. B **19**, 3827 (1986).
[12] J. Oreg, W. H. Goldstein, M. Klapisch, and A. Bar-Shalom, Phys. Rev. A **44**, 1750 (1991).
[13] M. S. Pindzola, D. C. Griffin, N. R. Badnell, and H. P. Summers, Nuclear Fusion Supplement **6**, 117 (1996).
[14] M. H. Chen, K. J. Reed, and D. L. Moores, Phys. Rev. Letts. **64**, 1350 (1990).
[15] J. Linkemann, A. Müller, J. Kenntner, D. Habs, D. Schwalm, A. Wolf, N. R. Badnell, and M. S. Pindzola, Phys. Rev. Letts. **74**, 4173 (1995).
[16] D. C. Griffin and M. S. Pindzola, J. Phys. B **21**, 3253 (1988).

```
seq ='Na'    nucch1 =26                                                    ADF23

  final level indexing       bwnf =  10178634.5     nprf =  5
  --------------------
  indf    code           S L   WJ       wnf
  ----    ----           - -   --  ------------
    1    2p63s0         (1)0( 0.0)          0.0
    2    2p53s1         (3)1( 2.0)    5848617.6
    3    2p53s1         (3)1( 1.0)    5863998.4
    4    2p53s1         (3)1( 0.0)    5950710.4
    5    2p53s1         (1)1( 1.0)    5960268.0

  initial level indexing     bwni =   3946116.3     nlev =  1
  --------------------
  indi    code           S L   WJ       wni
  ----    ----           - -   --  ------------
    1    2p63s1         (2)0( 0.5)          0.0

------------------------------------------------------------------------------
meti*= 1

  ionis rates
  -----------
  indf Te= 5.12E+05  1.28E+06  2.56E+06  5.12E+06  1.28E+07  2.56E+07  5.12E+07  1.28E+08  2.56E+08  5.12E+08  1.28E+09  2.56E+09
  ---- ---
    1      1.20E-15  1.28E-12  1.39E-11  4.63E-11  9.15E-11  1.07E-10  1.06E-10  8.99E-11  7.43E-11  5.93E-11  4.26E-11  3.26E-11
    2      4.42E-23  1.06E-15  3.41E-13  6.55E-12  4.04E-11  7.32E-11  9.40E-11  9.77E-11  8.86E-11  7.53E-11  5.71E-11  4.49E-11
    3      2.54E-23  6.27E-16  2.03E-13  3.92E-12  2.42E-11  4.39E-11  5.64E-11  5.87E-11  5.32E-11  4.52E-11  3.43E-11  2.70E-11
    4      6.63E-24  1.90E-16  6.45E-14  1.28E-12  8.02E-12  1.46E-11  1.89E-11  1.97E-11  1.78E-11  1.52E-11  1.15E-11  9.07E-12
    5      1.94E-23  5.63E-16  1.93E-13  3.82E-12  2.40E-11  4.39E-11  5.66E-11  5.90E-11  5.36E-11  4.56E-11  3.46E-11  2.72E-11

C  ---------------------------------------------------------------------------
C  Data generated by Donald C. Griffin   on   8/5/97
C
C  The rates were calculated using configuration-average ionization cross
C  sections, with semi-relativistic wavefunctions, using the
C  frozen-core approximation , the post form  for the scattering
C  potentials, and the maximum-interference approximation.
C  They were then multiplied by the appropriate angular coefficients.
C  ---------------------------------------------------------------------------
```

TABLE I. Maxwellian rate coefficients for direct ionization of Fe^{15+}.

```
seq ='Na'    nucch1 =26                                                    ADF23

  final level indexing       bwnf =  10164840.0     nprf =  1
  --------------------
  indf    code           S L   WJ       wnf
  ----    ----           - -   --  ------------
    1    2p63s0         (1)0( 0.0)          0.0

  initial level indexing     bwni =   3942587.8     nlev =  1
  --------------------
  indi    code           S L   WJ       wni
  ----    ----           - -   --  ------------
    1    2p63s1         (2)0( 0.5)          0.0

------------------------------------------------------------------------------
meti*= 1

  idion rates
  -----------
  indf Te= 5.12E+05  1.28E+06  2.56E+06  5.12E+06  1.28E+07  2.56E+07  1.28E+08
  ---- ---
    1      6.20E-19  7.02E-13  2.01E-11  9.88E-11  2.23E-10  2.71E-10  2.38E-10

C------------------------------------------------------------------------------
C
C  Data generated by Dario M. Mitnik on 9/25/97
C
C  The rates were calculated using the HULLAC code
C  This code uses atomic many-electron relativistic wave
C  functions. For the Distorted-Wave collisional excitation
C  cross-sections, the Factorization-Interpolation method
C  is used.
C
C
C  The following intermediate inner-shell excited
C  configurations were included in the calculation:

C   p53s  p53p  p53d  p54s  p54p
C   p54d  p54f  p55s  p55p  p55d
C   p55f  p55g  p56s  p56p  p56d
C   p56f  p56g  p56h  s13s  s13p
C   s13d  s14s  s14p  s14d  s14f
C
C------------------------------------------------------------------------------
C
```

TABLE II. Maxwellian rate coefficients for excitation-autoionization of Fe^{15+}.

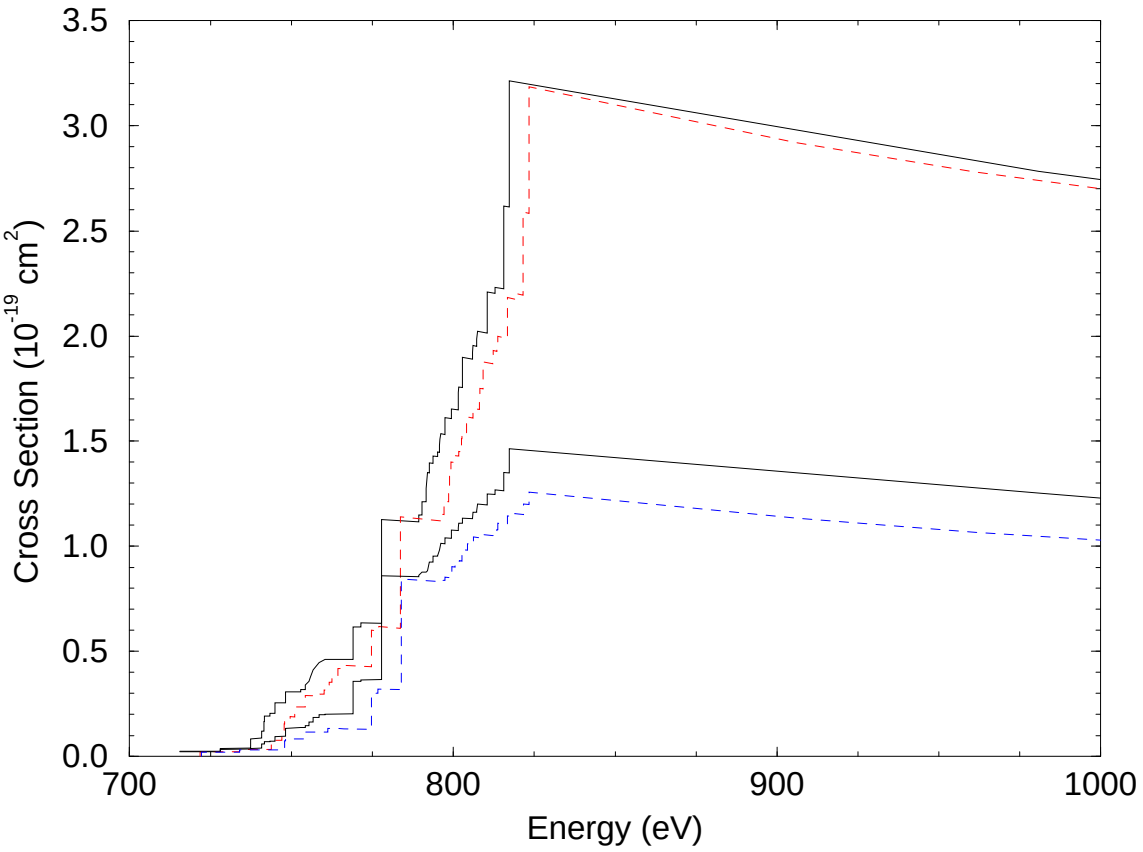

FIG. 1. Excitation-autoionization cross sections for Fe^{15+}, including only the $2p \rightarrow 3\ell$ transitions. Upper solid curve: fully-relativistic without radiation damping, lower solid curve: fully-relativistic with radiation damping, upper dashed curve: perturbative-relativistic without radiation damping, lower dashed curve: perturbative-relativistic with radiation damping.

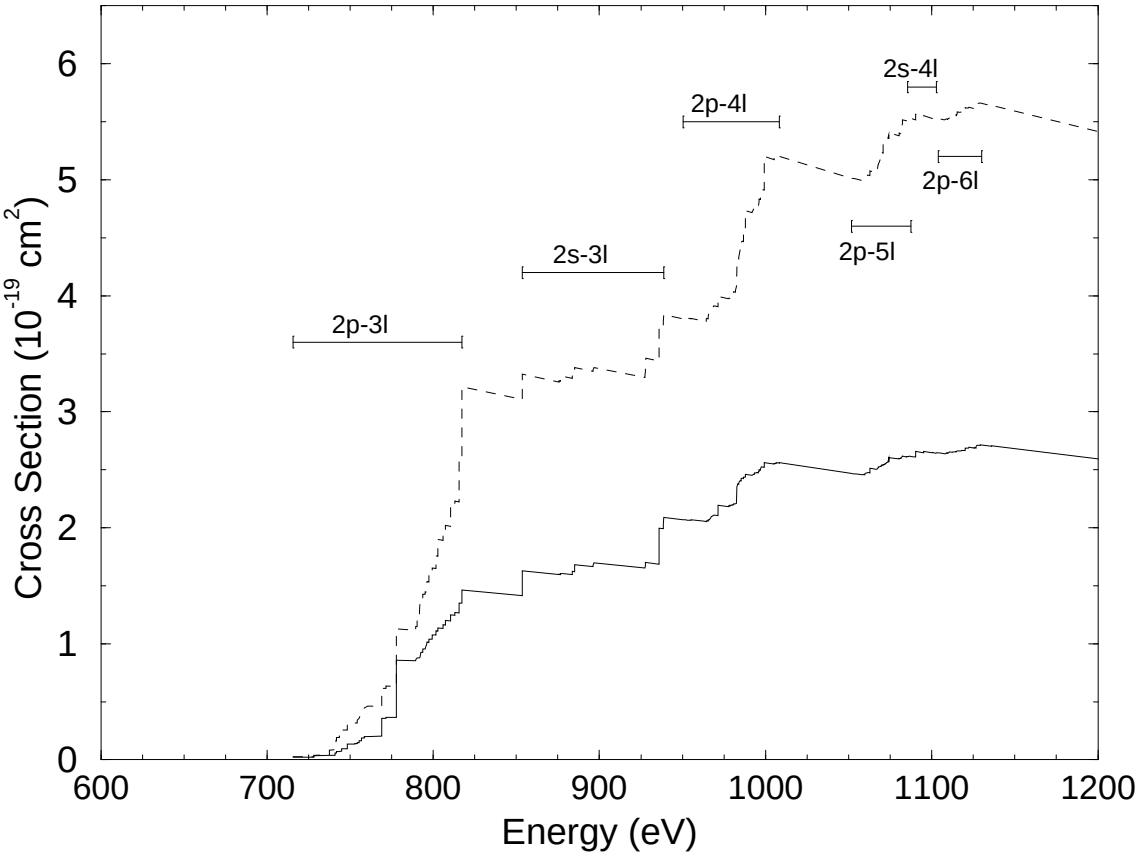

FIG. 2. Excitation-autoionization cross sections for Fe^{15+}, including the $2p \rightarrow n\ell (n = 3, 4, 5, 6)$ and $2s \rightarrow n\ell (n = 3, 4)$ transitions. Dashed curve: fully-relativistic without radiation damping, solid curve: fully-relativistic with radiation damping.

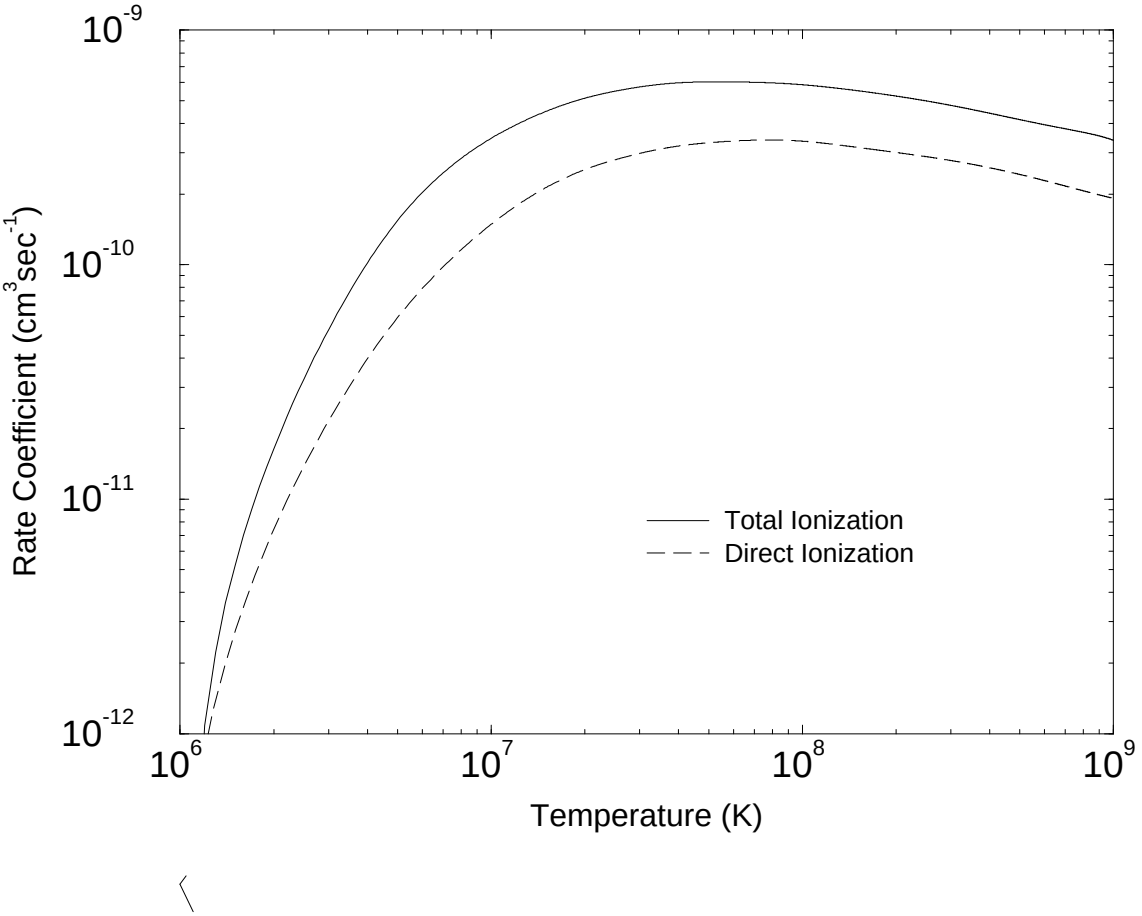

FIG. 3. Maxwellian rate coefficients for Fe^{15+}. Solid curve: total ionization, dashed curve: direct ionization only.